APERTURE ANTENNAS

Aperture antennas are most commonly used in the microwave- and millimeter-wave frequencies. There are a large number of antenna types for which the radiated electromagnetic fields can be considered to emanate from a physical aperture. Antennas that fall into this category include several types of reflectors: planar (flat plate) arrays, lenses, and horns. The geometry of the aperture geometry may be square, rectangular, circular, elliptical, or virtually any other shape. Aperture antennas are very popular for aerospace applications because they can be flush mounted onto the spacecraft or aircraft surface. Their opening can be covered with an electromagnetic (dielectric) window material or radome to protect the antenna from environmental conditions (1). This installation will not disturb the aerodynamic profile of the vehicle, which is of critical importance in high-speed applications.

In order to evaluate the distant (far-field) radiation patterns, it is necessary to know the internal currents that flow on the radiating surfaces. However, these current distributions may not be exactly known and only approximate or experimental measurements can provide estimates for these data. To expedite the process, it is necessary to have alternative methods to compute the radiation patterns of the aperture antennas. A technique based on the equivalence principle allows one to make a reasonable approximation to the fields on, or in the vicinity of, the physical antenna structure and subsequently to compute the radiation patterns.

Field *equivalence,* first introduced by Schelkunoff (2), is a principle by which the actual sources on an antenna are replaced by equivalent sources on an external closed surface that is physically outside of the antenna. The fictitious sources are said to be equivalent within a region because they produce the same fields within that region. Another key concept is Hugens's principle (3), which states that the equivalent source at each point on the external surface is a source of a spherical wave. The secondary wave front can be constructed as the envelope of these secondary spherical waves (4).

Using these principles, the electrical and/or magnetic fields in the equivalent aperture region can be determined with straightforward approximate methods. The fields elsewhere are assumed to be zero. In most applications, the closed surface is selected so that most of it coincides with the conducting parts of the physical structure. This is preferred because the vanishing of the tangential electrical components over the conducting parts of the surface reduces the physical limits of integration. The formula to compute the fields radiated by the equivalent sources is exact, but it requires integration over the closed surface. The degree of accuracy depends on the knowledge of the tangential components of the fields over the closed surface.

Aperture techniques are especially useful for parabolic reflector antennas, where the aperture plane can be defined immediately in front of the reflector. Parabolic reflectors are usually large, electrically. More surprisingly, aperture techniques can be successfully applied to small aperture waveguide horns. However, for very small horns with an aperture dimension of less than approximately one wavelength, the assumption of zero fields outside the aperture fails unless the horn is surrounded by a planar conducting flange (5). In this section, the mathematical formulas will be developed to analyze the radiation characteristics of aperture antennas. Emphasis will be given to the rectangular and circular configurations because they are the most commonly used geometries. Due to mathematical complexities, the results will be restricted to the far-field region.

One of the most useful concepts to be discussed is the far-field radiation pattern that can be obtained as a Fourier transform of the field distribution over the equivalent aperture, and vice versa. The existing relationship of the Fourier transforms theory is extremely important since it makes all of the operational properties of the Fourier transform theory available for the analysis and synthesis of aperture antennas. Obtaining analytical solutions for many simple aperture distributions in order to design aperture antennas is useful. More complex aperture distributions, which do not lend themselves to analytical solutions, can be solved numerically. The increased capabilities of the personal computer (PC) have resulted in its acceptance as a conventional tool of the antenna designer. The Fourier-transform integral is generally well behaved and does not present any fundamental computational problems.

Considering the use of the Fourier transform, first consider rectangular apertures in which one aperture dimension is large in wavelength and the other is small in terms of wavelength. This type of aperture is approximated as a line source and is easily treated with a one-dimensional Fourier transform (6). For many kinds of rectangular aperture antennas such as horns, the aperture distributions in the two principal plane dimensions are independent. These types of distributions are said to be separable. The total radiation pattern is obtained for separable distributions as the product of the pattern functions obtained from a one-dimensional Fourier transform, which corresponds to the two principal plane distributions.

If the rectangular aperture distribution is not able to be separated, the directivity pattern is found in a similar manner to the line-source distribution except that the aperture

field is integrated over two dimensions rather than one dimension (7). This double Fourier transform can also be applied to circular apertures and can be easily evaluated on a PC.

For all aperture distributions, the following observations are made (8):

1. A uniform amplitude distribution yields the maximum directivity (nonuniform edge-enhanced distributions for supergain being considered impractical), but at high side-lobe levels.
2. Tapering the amplitude at the center, from a maximum to a smaller value at the edges, will reduce the side-lobe level compared with the uniform illumination, but it results in a larger (main-lobe) beam width and less directivity.
3. An inverse-taper distribution (amplitude depression at the center) results in a smaller (main-lobe) beam width but increases the side-lobe level and reduces the directivity when compared with the uniform illumination case.
4. Depending on the aperture size in wavelengths and phase error, there is a frequency (or wavelength) for which the gain peaks, falling to smaller values as the frequency is either raised or lowered.

Lastly, we consider aperture efficiencies. The *aperture efficiency* is defined as the ratio of the effective aperture area to the physical aperture area. The *beam efficiency* is defined as the ratio of the power in the main lobe to the total radiated power. The maximum aperture efficiency occurs for a uniform aperture distribution, but maximum beam efficiency occurs for a highly tapered distribution. The aperture phase errors are the primary limitation of the efficiency of the antenna.

HUYGENS'S PRINCIPLE

The principle proposed by Christian Huygens (1629–1695) is of fundamental importance in the development of the wave theory. Huygens's principle states that, "Each point on a primary wavefront serves as the source of spherical secondary wavelets that advance with a speed and frequency equal to those of the primary wave. The primary wavefront at some later time is the envelope of these wavelets" (9,10). This is illustrated in Fig. 1 for spherical and plane waves modeled as a construction of Huygens secondary waves. Actually, the intensities of the secondary spherical wavelets are not uniform in all directions, but vary continuously from a maximum in the direction of wave propagation to a minimum of zero in the backward direction. As a result, there is no backward propagating wavefront. The Huygens source approximation is based on the assumption that the magnetic and electrical fields are related as a plane wave in the aperture.

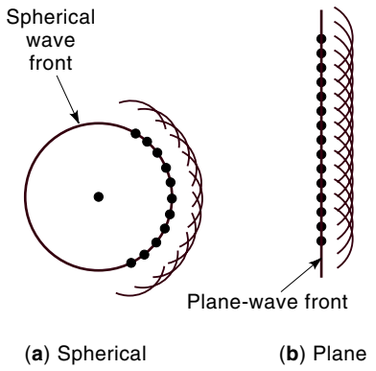

Figure 1. Spherical and plane-wave fronts constructed with Huygens secondary waves.

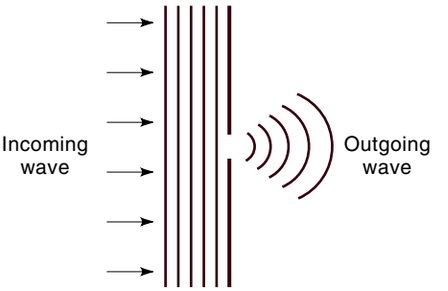

Figure 2. Diffraction of waves through a slit based on the Huygens principle.

Let us consider the situation shown in Fig. 2, in which an infinite electromagnetic plane wave is incident on an infinite flat sheet that is opaque to the waves. This sheet has an opening that is very small in terms of wavelengths. Accordingly, the outgoing wave corresponds to a spherical wavefront propagating from a point source. That is, when an incoming wave comes against a barrier with a small opening, all but one of the effective Huygens point sources are blocked, and the energy coming through the opening behaves as a single point source. In addition, the outgoing wave emerges in all directions, instead of just passing straight through the slit.

On the other hand, consider an infinite plane electromagnetic wave incident on an infinite opaque sheet shown in Fig. 3 that has an opening a. The field everywhere to the right of the sheet is the result of the section of the wave that passes through the slot. If a is large in terms of wavelengths, the field distribution across the slot is assumed, to a first approximation, to be uniform. The total electromagnetic field at a point to the right of the opening is obtained by integrating the contributions from an array of Huygens sources distributed over the length a. We calculate the electrical field at point P on a reference plane located at a distance R_0 behind

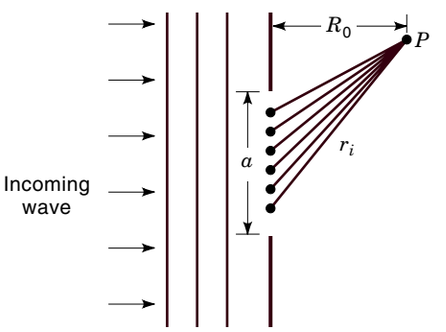

Figure 3. Plane wave incident on an opaque sheet with a slot of width a.

the plane by Huygens's principle (11):

$$E = \int E_0 \frac{e^{-jkr}}{r}\, dy \tag{1}$$

For points near to the array, the integral does not simplify but can be reduced to the form of Fresnel integrals.

The actual evaluation of this integral is best achieved on a PC computer, which reduces the integral to the summation of N Huygens sources:

$$E = \sum_{i=1}^{N} E_0 \frac{e^{-jkr_i}}{r_i} \tag{2}$$

where r_i is the distance from the ith source to point P. The field variation near the slot that is obtained in this way is commonly called a *Fresnel diffraction pattern* (4).

For example, let us consider the case in which the slot length a is 5 cm and the wavelength is 1.5 cm (20 GHz). We can use Eq. (2) to compute the field along a straight line parallel to the slot and distance R_0 from it. The field variation for R_0 = 2.5 cm shown in Fig. 4(a) is well within the near field (Fresnel region). As we continue to increase R_0 the shape of the field variation along this line continues to vary with R_0 until we reach the far field or Fraunhofer region. [See the trends in Figs. 4(b), 4(c), and 4(d)]. Once we have entered the Fraunhofer region, the pattern is invariant to range. For the point to be in the far field, the following relationship must exist:

$$R_0 \geq \frac{2a^2}{\lambda} \tag{3}$$

where a is the width of the slot and λ is the wavelength. Thus, the larger the aperture or the shorter the wavelength, the greater the distance at which the pattern must be measured if we wish to avoid the effects of Fresnel diffraction.

Huygens's principle is not without limitations as it neglects the vector nature of the electromagnetic field space. It also neglects the effect of the currents that flow at the slot edges. However, if the aperture is sufficiently large and we confine our attention to directions roughly normal to the aperture, the scalar theory of Huygens's principle gives very satisfactory results.

Geometric optic techniques are commonly applied in reflector antennas to establish the fields in the reflector aperture plane. This procedure is referred to as the *aperture field method* and it is employed as an alternative to the so-called induced current method, which is based upon an approximation for the electric current distribution on the reflector surface. The fields in the aperture plane can be thought of as an ensemble of Huygens sources. The radiation pattern can be computed via a numerical summation of the sources.

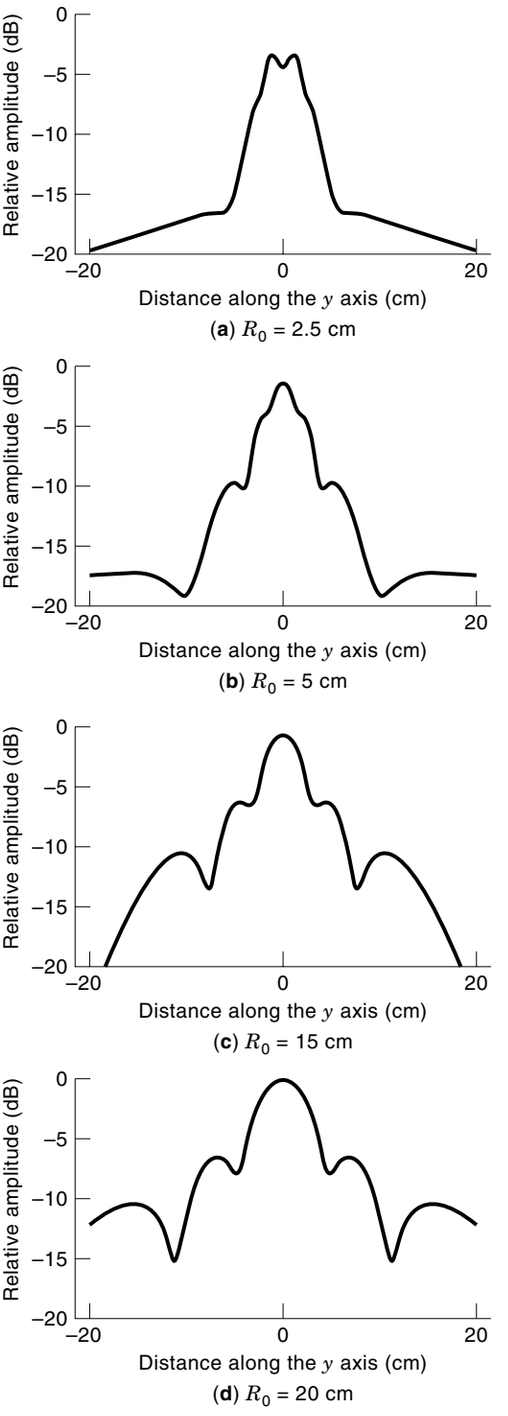

Figure 4. Electromagnetic field versus distance along the Y axis.

EQUIVALENCE PRINCIPLE

The ability to determine electromagnetic waves radiated fields via *field-equivalence principles* is a useful concept and the development can be traced back to Schelkunoff (2). The equivalence principle often makes an exact solution easier to obtain or suggests approximate methods that are of value in simplifying antenna problems. Field-equivalence principles are treated at length in the literature and we will not consider the many variants here. The book by Collin and Zucker (12) is a useful source of references in this respect. The basic concept is illustrated in Fig. 5. The electromagnetic source region is enclosed by a surface S that is sometimes referred to as Huygens's surface.

In essence, Huygens's principle and the equivalence theorem shows how to replace actual sources by a set of equivalent sources spread over the surface S (13). The equivalence principle is developed by considering a radiating source, electrically represented by current densities $\boldsymbol{J}_1$ and $\boldsymbol{M}_1$. Assume that the source radiates fields $\boldsymbol{E}_1$ and $\boldsymbol{H}_1$ everywhere. We would like to develop a method that will yield the fields outside the closed surface. To accomplish this, a closed surface S is shown by the dashed lines that enclose the current densities $\boldsymbol{J}_1$ and $\boldsymbol{M}_1$. The volume inside S is denoted by V. The primary task is to replace the original problem [Fig. 5(a)] by an equivalent one that will yield the same fields $\boldsymbol{E}_1$ and $\boldsymbol{H}_1$ [Fig. 5(b)]. The formulation of the problem can be greatly aided if the closed surface is judiciously chosen so that the fields over most of the surface, if not the entire surface, are known a priori.

The original sources $\boldsymbol{J}_1$ and $\boldsymbol{M}_1$ are removed, and we assume that there exists a field $\boldsymbol{E}$ and $\boldsymbol{H}$ inside V. For this field to exist within V, it must satisfy the boundary conditions on the tangential electrical and magnetic field components on surface S. Thus on the imaginary surface S, there must exist equivalent sources (14):

$$\boldsymbol{J}_S = \boldsymbol{n} \times (\boldsymbol{H}_1 - \boldsymbol{H}) \tag{4}$$

$$\boldsymbol{M}_S = -\boldsymbol{n} \times (\boldsymbol{E}_1 - \boldsymbol{E}) \tag{5}$$

These equivalent sources radiate into an *unbounded* space. The current densities are said to be equivalent only outside region V, because they produce the original field ($\boldsymbol{E}_1$, $\boldsymbol{H}_1$). A field $\boldsymbol{E}$ or $\boldsymbol{H}$, different from the original, may result within V.

The sources for electromagnetic fields are always, apparently, electrical currents. However, the electrical current distribution is often unknown. In certain structures, it may be a complicated function, particularly for slots, horns, reflectors, and lenses. With these types of radiators, the theoretical work is usually not based on the primary current distributions. Rather, the results are obtained with the aid of what is known as *aperture theory* (15). This simple, sound theory is based upon the fact that an electromagnetic field in a source-free, closed region is completely determined by the values of tangential $\boldsymbol{E}$ or tangential $\boldsymbol{H}$ on the surface of the closed region. For exterior regions, the boundary condition at infinity may be employed, in effect, to close the region. This is exemplified by the following case.

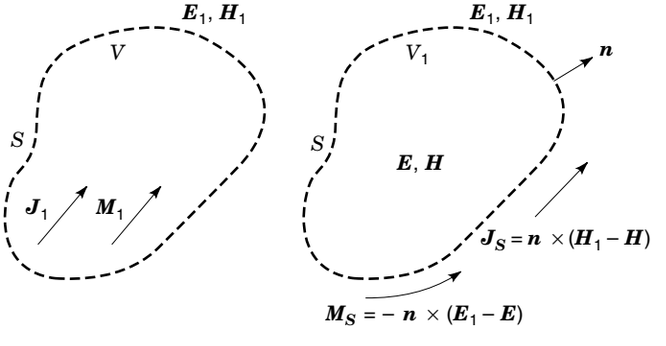

Figure 5. Equivalence principle with a closed Huygens surface S enclosing sources.

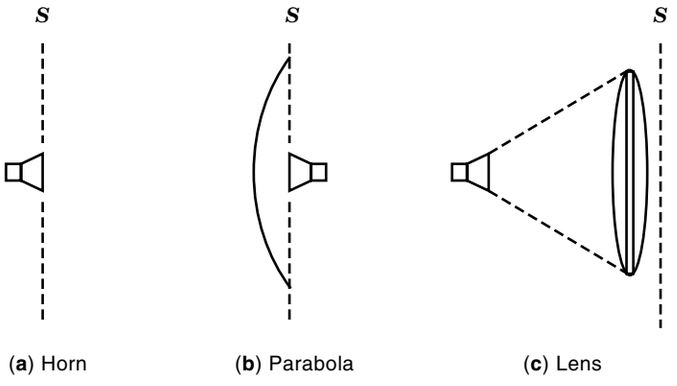

Figure 6. Some apertures yielding the same electromagnetic fields to the right side of the Huygens surface S.

Without changing the $\boldsymbol{E}$ and $\boldsymbol{H}$ fields external to S, the electromagnetic source region can be replaced by a zero-field region with appropriate distributions of electrical and magnetic currents ($\boldsymbol{J}_s$ and $\boldsymbol{M}_s$) on the Huygens surface. This example is overly restrictive and we could specify any field within S with a suitable adjustment. However, the zero internal field approach is particularly useful when the tangential electrical fields over a surface enclosing the antenna are known or can be approximated. In this case, the surface currents can be obtained directly from the tangential fields, and the external field can be determined.

Assuming zero internal field, we can consider the electromagnetic sources inside S to be removed, and the radiated fields outside S are then determined from the electrical and magnetic surface current distributions alone. This offers significant advantages when the closed surface is defined as a two-hemisphere region, with all sources contained on only one side of the plane. If either the electrical or magnetic fields arising from these sources can be determined over the planar Huygens surface S, then the radiated fields on the far side of the plane can be calculated. The introduction of an infinite conducting sheet just inside the Huygens surface here will not complicate the calculations of the radiated fields in the other half-space (16). This infinite-plane model is useful for antennas the radiation of which is directed into the right hemisphere (Fig. 6), and has found wide application in dealing with aperture antennas. For instance, if the antenna is a rectangular horn, it is assumed the horn transitions into a infinite flange. All tangential fields outside the rectangular boundary along the infinite Huygens surface are taken to be zero.

When the limitations of the half-space model are acceptable, it offers the important advantage that either the electrical or magnetic currents need to be specified. However, knowledge of both is not required. It must be emphasized that any of the methods described before will produce exact results over the Huygens surface.

In the analysis of electromagnetic problems, often it is easier to form equivalent problems that will yield the same solution only within a region of interest. This is the case for aperture antenna problems.

The steps that must be used to form an equivalent problem and solve an aperture antenna problem are as follows:

1. Select an imaginary surface that encloses the actual sources (the aperture). The surface must be judiciously chosen so that the tangential components of the electrical field and/or the magnetic field are known, exactly or approximately, over its entire span. Ideally, this surface is a flat plane extending to infinity.
2. Over the imaginary surface, form equivalent current densities $\boldsymbol{J}_S$ and $\boldsymbol{M}_S$ over S, assuming that the $\boldsymbol{E}$ and $\boldsymbol{H}$ fields within S are not zero.
3. Lastly, solve the equivalent-aperture problem.

RECTANGULAR APERTURES

There are many kinds of antennas for which the radiated electromagnetic fields emanate from a physical aperture. This general class of antennas provides a very convenient basis for analysis and permits a number of well-established mathematical techniques to be applied that provides expressions for the distant radiation fields.

Horns or parabolic reflectors, in particular, can be analyzed as aperture antennas. Incident fields are replaced by equivalent electrical and magnetic currents. With use of vector potentials, the far fields are found as a superposition of each source. Generally one can assume that the incident field is a propagating free-space wave, the electrical and magnetic fields of which are proportional to each other. This will give the Huygens source approximation and allow us to use integrals of the electric field in the aperture. Each point in the aperture is considered a source of radiation.

The first step involved in the analysis of aperture antennas is to calculate the electromagnetic fields over the aperture due to the sources on the rearward side of the infinite plane and to use these field distributions as the basis for the prediction of the distant fields in the forward half-space. The electromagnetic fields in the aperture plane cannot be determined exactly but approximation distributions can be found by many different methods, which are dependent upon the antenna. One can find the far-field radiation pattern for various distributions by a Fourier-transform relation.

For instance, consider a line source of length L_w using the coordinate system as illustrated in Fig. 7. Assume that the source is positioned in a ground plane of infinite extent. This model is simple and yet the analysis gives results that illustrate the main features of the most practical of the two-dimensional apertures. The line-source distribution does have a practical realization, namely, in a long one-dimensional array that has sufficient elements to enable it to be approximated to a continuous distribution. The applicable transform pair is (7,17)

$$E(\sin\theta) = \int_{-\infty}^{\infty} E(x) e^{jkx \sin\theta}\, dx \tag{6}$$

and

$$E(x) = \int_{-\infty}^{\infty} E(\sin\theta) e^{jkx \sin\theta} d(\sin\theta) \tag{7}$$

where $k = 2\pi/\lambda$. For real values of θ, $-1 \le \sin\theta \le 1$, the field distribution represents radiated power, while outside this region it represents reactive or stored power (18). The field distribution $E(\sin\theta)$, or an angular spectrum, refers to an angular distribution of plane waves. The angular spectrum for a finite aperture is the same as the far-field pattern, $E(\theta)$. Thus, for a finite aperture the Fourier integral representation of Eq. (6) may be written (8):

$$E(\theta) = \int_{+L_w/2}^{-L_w/2} E(x) e^{jkx \sin\theta}\, dx \tag{8}$$

Note that Eq. (8) is a relative relation.

For example, consider a uniform distribution for which

$$E(x) = \frac{1}{L_w} \tag{9}$$

The field distribution pattern can be found by incorporating this into Eq. (8):

$$E(\theta) = \frac{1}{L_w} \int_{-L_w/2}^{L_w/2} e^{(j2\pi x/\lambda)\sin\theta}\, dx \tag{10}$$

We complete the straightforward integration to get the final result:

$$E(\theta) = \frac{\sin\left(\dfrac{\pi L_w}{\lambda}\sin\theta\right)}{\dfrac{\pi L_w \sin\theta}{\lambda}} \tag{11}$$

This $\sin(x)/x$ distribution is very important in antenna theory and is the basis for many antenna designs. It has a first sidelobe level of -13.2 dB.

Another popular continuous aperture distribution is the cosine raised to power n,

$$E(x) = \cos^n\left(\frac{\pi}{L_w}x\right) \tag{12}$$

where $-L_w/2 \le x \le L_w/2$. This is shown in Fig. 8 for $n = 0$, 1, 2, and 3. To make a relative comparison of the various distributions, we must first normalize to the transmitted power of the uniform case. To do this, we multiply the pattern function

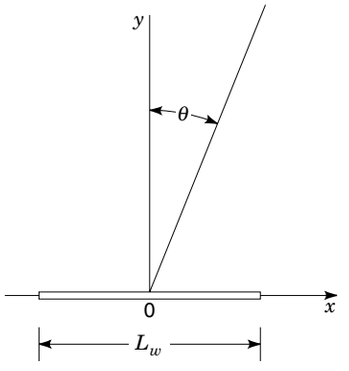

Figure 7. Coordinate system used to analyze a linear aperture of length L_w.

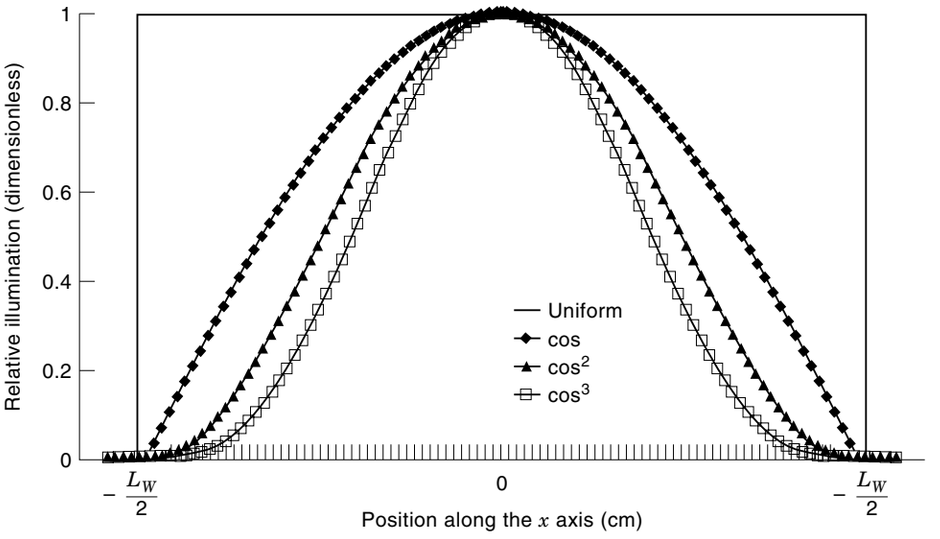

Figure 8. Some popular aperture distributions.

by the normalization constant:

$$Cp = \frac{1}{\int_{-L_w/2}^{L_w/2} E^2(x)\,dx} \tag{13}$$

To demonstrate the principles, we computed the antenna radiation pattern of a 1 meter long line-source antenna for cosine^0 (uniform), cosine^1, and cosine^2 distributions. The operating wavelength is 3 cm. The resulting patterns are shown in Fig. 9. These data indicate that the more heavily tapered illuminations result in decreased side-lobe levels, but at a penalty of main beam peak gain.

Many distributions actually obtained in practice can be approximated by one of the simpler forms or by a combination of simple forms. For example, a common linear aperture distribution is the cosine on a pedestal p:

$$E(x) = p + (1-p)\cos\left(\frac{\pi x}{L_w}\right) \tag{14}$$

where $0 \le p \le 1$. This is a combination of a uniform plus a cosine type distribution. The triangular distribution is popular:

$$E(x) = 1 + \frac{x}{L_w/2} \tag{15}$$

for $-L_w/2 \le x \le 0$, and

$$E(x) = 1 - \frac{x}{L_w/2} \tag{16}$$

for $0 \le x \le L_w/2$.

In practice, the rectangular aperture is probably the most common microwave antenna. Because of its configuration, the rectangular coordinate system is the most convenient system to express the fields at the aperture. The most common and convenient coordinate system used to analyze a rectangular aperture is shown in Fig. 10. The aperture lies in the x–y plane and has a defined tangential aperture distribution $E(x, y)$. In keeping with the equivalence principle we shall assume

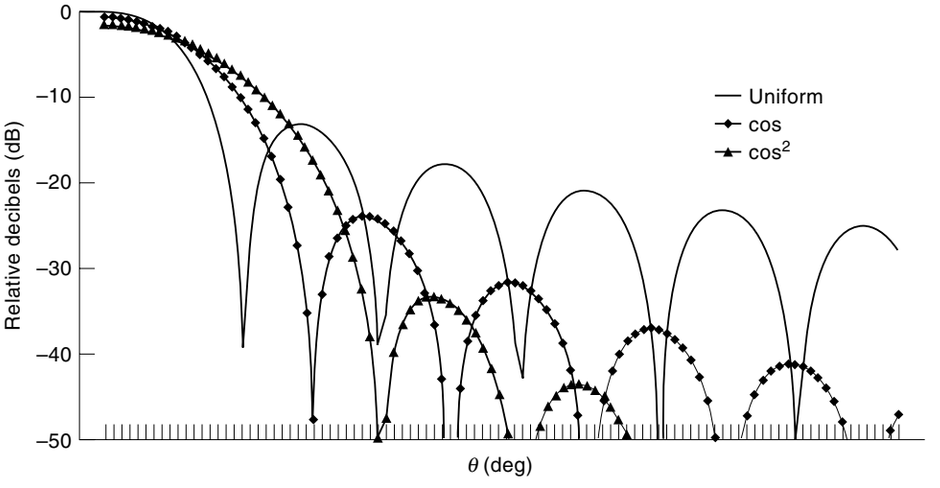

Figure 9. Radiation patterns of line sources for three different aperture distributions (L_w = 1 m, λ = 3 cm).

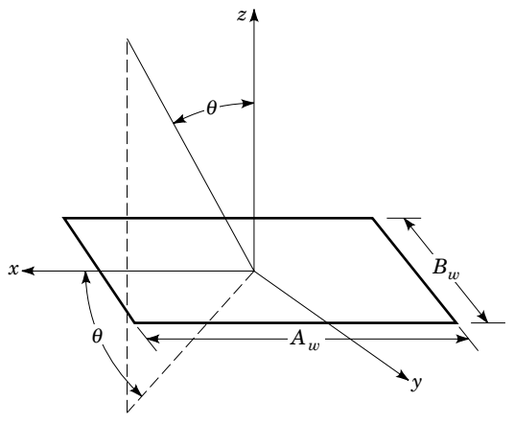

Figure 10. Coordinate system used to analyze rectangular aperture of dimensions A_w, B_w.

the x–y plane is a closed surface that extends from $-\infty$ to $+\infty$ in the x–y plane. Outside the rectangular aperture boundaries we shall assume that the field distribution is zero for all points on this infinite surface. The task is to find the fields radiated by it, the pattern beam widths, the side-lobe levels of the pattern, and the directivity.

Note that a horn of aperture size A_w by B_w, with $A_w/\lambda \gg 1$ and $B_w/\lambda \ll 1$, can be analyzed as a *continuous* line source. If these conditions are not met, the pattern must be obtained by the integral (19):

$$E(\theta, \phi) = \int_{B_w/2}^{-B_w/2} \int_{A_w/2}^{-A_w/2} E(x, y) e^{j(k_x x + k_y y)}\, dx\, dy \qquad (17)$$

where

$k_x = k \sin\theta \cos\phi$
$k_y = k \sin\theta \sin\phi$

These are the x and y components of the propagation vector $\boldsymbol{k}$ (20).

For many types of antennas, such as the rectangular horn, the x and y functions are separable and may be expressed by the form

$$E(x, y) = E(x)E(y) \qquad (18)$$

For this particular distribution, the pattern in the principal x–z plane can be determined from a line-source distribution $E(x)$ while the pattern in the y–z plane can be determined from a line-source distribution $E(y)$.

We use the Fourier transform and ignore the polarization of the electric field in the aperture to get the result

$$E(k_x, k_y) = \frac{\sin\left(k_x \frac{A_w}{2}\right)}{k_x \frac{A_w}{2}} \frac{\sin\left(k_y \frac{B_w}{2}\right)}{k_y \frac{B_w}{2}} \qquad (19)$$

This pattern in both planes is given by a $\boldsymbol{k}$-space function. We conclude that the result quoted for a line-source distribution applies for the principal planes of separable rectangular antenna apertures.

For nonseparable distributions, the integration of Eq. (17) is best carried out on a PC computer using numerical methods. Figure 11 is a listing of a simple program written in Basic that can be run on any PC computer.

In running the program, $\phi = 0$ corresponds to the principal plane pattern in the x–z plane while $\phi = 90°$ is the principal plane pattern in the y–z plane. For example, consider an aperture with $A_w = 75$ cm, $B_w = 125$ cm, and $\lambda = 3$ cm. Assume cosine distribution in each plane. The principal plane patterns in the x plane and y plane and the pattern in the intercardinal plane ($\theta = 45°$) that result are shown in Fig. 12.

We applied the computer code to compute the secondary pattern characteristic produced by uniform, cosine raised to power n, cosine on a pedestal p, and triangular aperture distributions. The results shown in Table 1 compare the gain, beam width, and the first side-lobe levels. All gain levels are compared with the uniform illumination case.

A uniform line-source or rectangular aperture distribution produces the highest directivity. However, the first side lobe is only about -13.2 dB down. Thus, aperture distributions used in practice must be a trade-off or a compromise between the desired directivity (or gain) and side-lobe level.

CIRCULAR APERTURES

Circular antennas form the largest single class of aperture antennas. For instance, the circular parabolic reflector is used extensively in telecommunications and radar applications.

The most common and most convenient coordinate system used to analyze the radiation from a circular aperture of diameter D_w is shown in Fig. 13. The radiation field pattern for a circular aperture can be calculated by applying Huygens's principle in a similar way to that for a rectangular aperture (*a*). The simplest form of a circular aperture distribution is one in which the field does not vary with ϕ, that is, one that is rotationally symmetric. This is not always true in practice; however, we will assume that case here in order to demonstrate the methodology of analyzing circular apertures.

As was the case with rectangular apertures, a Fourier-transform relationship exists between the antenna distribution and the far-field radiation pattern. For a circular symmetric aperture distribution, the radiation pattern can be written in normalized form (6):

$$E(u) = \frac{1}{\pi^3} \int_0^{2\pi} \int_0^{\pi} E(P) e^{jPu\cos(\phi - \phi')} P\, dP\, d\phi' \qquad (20)$$

where

$$u = \frac{D_w \sin\theta}{\lambda}$$

and the normalized radius is

$$P = \frac{2\pi r}{D_w}$$

For a uniformly illuminated circular aperture, the normalized field pattern as a function of θ and D_w is (8)

$$E(u) = \frac{2J_1(\pi u)}{\pi u} \qquad (21)$$

```
CLS
‘Program to compute rectangular aperture radiation patterns
REDIM A(101, 101), patternx(200), patterny(200), intercardinal(200)
PI = 3.14159265358#
‘Results stored in file Rect.dat
OPEN ‘‘Rect.dat’’ FOR OUTPUT AS #1
‘------ input data ------
frequency = 10
Aw = 75: Bw = 125
‘---------------------
wavelength = 30 / frequency
Awave = Aw / wavelength: Bwave = Bw / wavelength
‘Load aperture distribution: all dimensions in cm
FOR I = 1 TO 101
FOR J = 1 TO 101
X = Aw * (51 - I) / 100: Y = Bw * (51 - J) / 100
A(I, J) = COS(PI * X / Aw) * COS(PI * Y / Bw)
‘Note: a(I, J) is the aperture distribution in the X and Y plane
NEXT J
NEXT I
‘Normalize power over aperture to that in a uniform distribution
power = 0
FOR I = 1 TO 101
FOR J = 1 TO 101
power = power + A(I, J) ^ 2
NEXT J
NEXT I
power = power / 101 ^ 2 : power = SQR(power)
Cp = 1 / power
‘ Cp is the desired normalization constant
FOR phi = 0 TO 90 STEP 45
‘Note: Phi = 0 results in principal X-plane pattern
‘ Phi = 45 results in intercardinal plane pattern
‘ Phi = 90 results in principal Y-plane pattern
K = 0: G0DB = 0
FOR theta = 0 TO 10 STEP .1
PRINT ‘‘Computing for theta=’’; theta; ‘’ Phi=’’; phi
RE = 0: IM = 0
K = K + 1
‘Integration over aperture
FOR I = 1 TO 101
FOR J = 1 TO 101
X = Aw * (51 - I) / 100: Y = Bw * (51 - J) / 100
psi = (2 * PI * X / wavelength) * SIN(theta * PI / 180) * COS(phi * PI / 180)
psi = psi + (2 * PI * Y / wavelength) * SIN(theta * PI / 180) * SIN(phi * PI / 180)
RE = RE + A(I, J) * COS(psi)
IM = IM + A(I, J) * SIN(psi)
NEXT J
NEXT I
TMM = Cp * SQR(RE ^ 2 + IM ^ 2) / 101 ^ 2
IF theta = 0 THEN
G0DB = 20 * LOG(TMM) / LOG(10): GV = TMM
END IF
TOT = 20 * LOG(TMM) / LOG(10)
IF phi = 0 THEN patternx(K) = TOT
IF phi = 45 THEN intercardinal(K) = TOT
IF phi = 90 THEN patterny(K) = TOT
NEXT theta
NEXT phi
K = 0
FOR theta = 0 TO 10 STEP .1
K = K + 1
PRINT #1, K, patternx(K), intercardinal(K), patterny(K)
PRINT ‘‘Angle=’’; theta; ‘’ Ex=’’; patternx(K); ‘’ Exy=’’; intercardinal(K): ‘’ Ey=’’; patterny(K)
NEXT theta
Print ‘’’’
PRINT ‘‘Peak Gain G0 (dB)=’’; G0DB; ‘’ G0(voltage)=’’; GV; ‘’ G0(power)=’’; GV ^ 2
CLOSE #1
END
```

Figure 11. Computer program to compute a radiation pattern from a rectangular aperture.

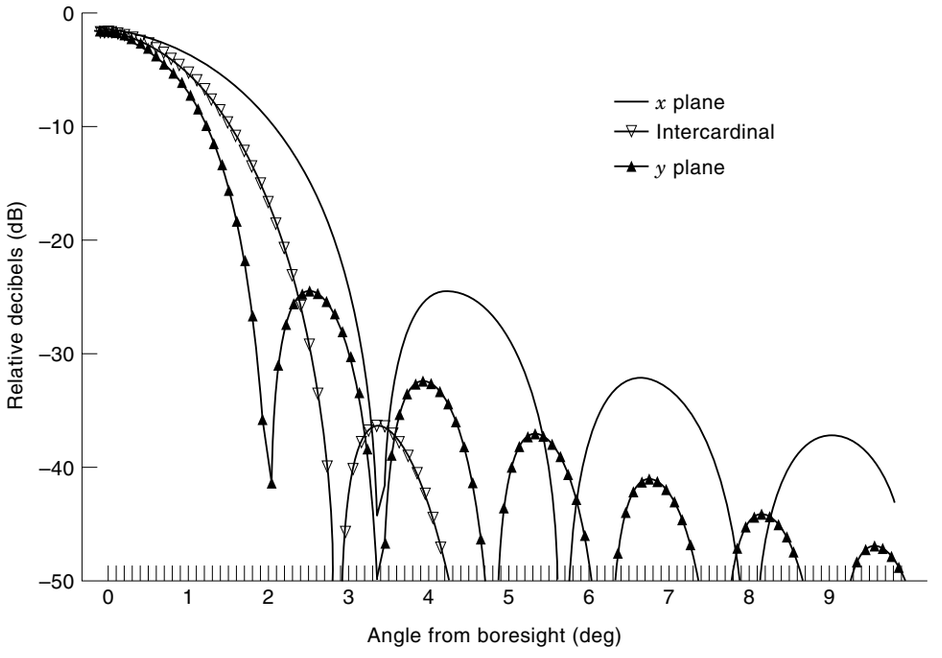

Figure 12. Radiation patterns for a rectangular aperture (A_w = 75 cm, B_w = cm, λ = 3 cm).

in which J_1 is a first-order Bessel function. This can also be expressed as

$$E(\theta) = \frac{2J_1\left(\frac{\pi D_w \sin\theta}{\lambda}\right)}{\frac{\pi D_w \sin\theta}{\lambda}} \tag{22}$$

The uniformly illuminated circular aperture radiation pattern has a first side-lobe level of −17.6 dB compared to −13.2 dB for that of the uniformly illuminated rectangular aperture.

Other types of circular aperture distributions include the cosine raised to power n:

$$E(r) = \cos^n\left(\frac{\pi r}{D_w}\right) \tag{23}$$

where $0 < r < D_w/2$.

The cosine on a pedestal p distribution is here defined:

$$E(r) = p + (1-p)\cos\left(\frac{\pi r}{D_2}\right) \tag{24}$$

Table 1. Radiation Pattern Characteristics Produced by Various Linear Aperture Distributions

Distribution	Comments	Normalized Half-Power Beam Width (deg) HPbw/K	Normalized Null-to-Null Beam Width (deg) NULLbw*/K	Side-Lobe Level (dB): SLL dB	Normalized Side-Lobe Angle (deg) SLpos/K	Gain Relative to Uniform (dB) G0 dB	Power Gain Factor Relative to Uniform G0 power	Voltage Gain Factor Relative to Uniform G0 volts
Uniform		50.67	114.67	−13.26	82.00	0.00	1.000	1.000
Cosine raised to power n	n = 1	68.67	172.00	−23.00	108.33	−0.91	0.810	0.900
	n = 2	82.67	229.33	−31.46	135.50	−1.76	0.666	0.816
	n = 3	95.33	286.67	−39.29	163.00	−2.40	0.576	0.759
	n = 4	106.00	344.00	−46.74	191.00	−2.89	0.514	0.717
	n = 5	116.67	402.00	−53.93	219.00	−3.30	0.468	0.684
Cosine on a pedestal p	p = 0.0	68.67	172.00	−23.01	108.33	−0.91	0.810	0.900
	p = 0.1	64.67	162.00	−23.00	98.00	−0.68	0.855	0.925
	p = 0.2	62.00	152.67	−21.66	97.00	−0.50	0.892	0.944
	p = 0.3	59.33	144.67	−20.29	93.67	−0.35	0.923	0.961
	p = 0.4	58.00	138.00	−18.92	90.67	−0.24	0.947	0.973
	p = 0.5	56.00	132.67	−17.65	88.33	−0.15	0.966	0.983
	p = 0.6	54.67	127.67	−16.53	86.67	−0.09	0.979	0.989
	p = 0.7	54.00	123.33	−15.55	85.00	−0.05	0.989	0.995
	p = 0.8	52.67	120.00	−14.69	83.83	−0.02	0.995	0.998
	p = 0.9	52.00	117.33	−13.93	82.67	−0.00	0.998	0.999
	p = 1.0	50.67	114.67	−13.26	82.00	0.00	1.000	1.000
Triangular		73.34	114.59	−26.52	164.00	−1.25	0.749	0.866

and the parabolic raised to a power n distribution (16) is

$$E(r) = \left[1 - \left(\frac{r}{D_w/2}\right)^2\right]^n \tag{25}$$

To analyze the various circular aperture distributions we can utilize a PC using numerical methods to perform the aperture integration. Actually a variant of the two-dimensional Fourier-transform relation used in the rectangular aperture analysis can be used. It works for any aperture rim shape including a circle. A listing of the program written in Basic appears in Fig. 14.

To demonstrate the behavior of various distributions, the computer code was applied to compare the secondary pattern characteristic produced by uniform, cosine raised to power n, cosine on a pedestal p, and parabolic raised to power n distributions. The results shown in Table 2 compare the gain, beam width, and the first side-lobe levels. All gain levels are compared with the uniform illumination case.

BEAM EFFICIENCY

This discussion considers the effect of the aperture field distribution on the beam and aperture efficiencies.

For many applications, the fraction of the total radiated energy that is in the main (null-to-null) antenna beam is important. This quantity is called the beam efficiency (21). The beam efficiency can be used to judge the ability of the antenna to discriminate between signals received through its main lobe and those through the minor lobes.

Before we go into this subject, it is helpful to review some fundamentals. The main beam is comprised of the solid angle

$$\Omega_M \approx \theta_{HP}\phi_{HP} \tag{26}$$

where θ_{HP} and ϕ_{HP} are the *half-power beam widths* (HPBW) in the two principal planes, minor lobes being neglected.

The (total) *beam area* Ω_A (or *beam solid angle* Ω_A) consists of the main-beam area (or solid angle) plus the minor-lobe area (or solid angle). Furthermore, the ratio of the main-beam area to the (total) beam area defines what is called the beam efficiency ϵ_M.

$$\epsilon_M = \frac{\Omega_M}{\Omega_A} \tag{27}$$

Using these symbols, the directivity of an antenna is given by

$$D = \frac{4\pi}{\Omega_A} = \frac{4\pi}{\lambda^2}A_p \tag{28}$$

where A_p is the physical area of the aperture. The *aperture efficiency* is defined as the ratio of the effective aperture area, A_e, to the physical aperture, or

$$\epsilon_{ap} = \frac{A_e}{A_p} \tag{29}$$

so that the ratio of the aperture and beam efficiencies is (8)

$$\frac{\epsilon_{ap}}{\epsilon_M} = \frac{A_e\Omega_A}{A_p\Omega_M} = \frac{k_0\lambda^2}{A_p\Omega_M} \tag{30}$$

where Ω_M is the main beam solid angle (sr), Ω_A the total beam solid angle (sr), and k_0 the free space wavenumbers ($k_0 = 2\pi/\lambda$). It is important to recognize, then, that beam efficiency and aperture efficiency are related to each other.

In terms of the radiated intensity $E(\theta, \phi)$ of a pencil beam with boresight at ($\theta = 0$, $\phi = 0$), the beam efficiency can be defined by (14)

$$n_B = \frac{\displaystyle\int_{-\theta_n}^{\theta_n}\int_{-\phi_n}^{\phi_n} E(\theta, \phi)E(\theta, \phi)^* \sin\theta\, d\phi\, d\theta}{\displaystyle\int_0^{\pi}\int_0^{2\pi} E(\theta, \phi)E(\theta, \phi)^* \sin\theta\, d\phi\, d\theta} \tag{31}$$

where θ_n is the angle from boresight to first null in θ and ϕ_n the angle from boresight to first null in ϕ. Also, $E(\theta, \phi)^*$ denotes the conjugate of $E(\sigma, \phi)$.

In general, the aperture and beam efficiencies must both be multiplied by a gain-degradation factor due to phase errors given by (22)

$$k_g = e^{-(2\pi\delta/\lambda)^2} \tag{32}$$

where δ is the rms phase error over the aperture. It is assumed that the correlation intervals of the deviations are greater than the wavelength. The controlling effect of the taper on the efficiencies (beam and aperture) tends to decrease as the phase error increases. The efficiencies are also reduced by the presence of the phase error.

The curves of Fig. 15 show that the beam efficiency tends to increase with an increase in taper but the aperture efficiency decreases. Maximum aperture efficiency occurs for a uniform aperture distribution, but maximum beam efficiency occurs for a highly tapered distribution. In most cases a taper is used that is intermediate between the two extremes.

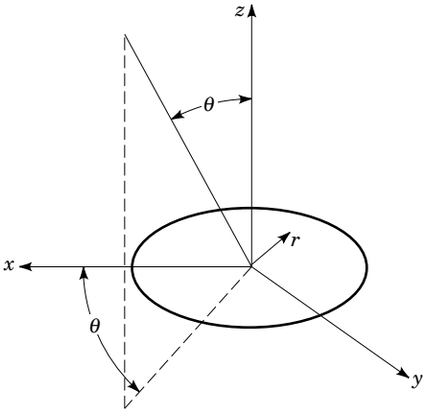

Figure 13. Coordinate system used to analyze a circular aperture of diameter D_w.

APERTURE SYNTHESIS

To simplify the discussion, we shall discuss a one-dimensional line source or length L_w. Earlier in Eqs. (6) and (7) a Fourier-

```
CLS
'Program to compute rectangular aperture radiation patterns
REDIM A(101, 101), pattern(200)
PI = 3.14159265358#
'Results stored in file Circ.dat
OPEN ''Circ.data'' FOR OUTPUT AS #1
'------ input data ------
frequency = 10: Dw = 100
'----------------------
wavelength = 30 / frequency: Dwave = Dw / wavelength
' Get reference power for uniformly illuminated circular array:
reference = 0
FOR I = 1 TO 101
FOR J = 1 TO 101
X = Dw * (51 - I) / 100: Y = Dw * (51 - J) / 100
radius = SQR(X ^ 2 + Y ^ 2)
IF radius > (Dw / 2) THEN
A(I, J) = 0
ELSE
A(I, J) = 1
END IF
reference = reference + A(I, J) ^ 2
NEXT J
NEXT I
'Load aperture distribution: all dimensions in cm
FOR I = 1 TO 101
FOR J = 1 TO 101
X = Dw * (51 - I) / 100: Y = Dw * (51 - J) / 100
radius = SQR(X ^ 2 + Y ^ 2)
IF radius > (Dw / 2) THEN
A(I, J) = 0
ELSE
A(I, J) = COS(PI * radius / Dw)
' Note: A(I, J) is aperture distribution in the X and Y plane
END IF
NEXT J
NEXT I
'Normalize power over aperture to that in a uniform distribution
power = 0
FOR I = 1 TO 101
FOR J = 1 TO 101
power = power + A(I, J) ^ 2
NEXT J
NEXT I
power = power / reference: power = SQR(power)
Cp = 1 / power
' Cp is the desired normalization constant
phi = 0
'Note: Phi=0 results in principal X-plane pattern
' Phi=45 results in intercardinal plane pattern
' Phi=90 results in principal Y-plane pattern
' For a symmetrical circular distribution, all these are the same
K = 0: G0DB = 0
FOR theta = 0 TO 10 STEP .1
PRINT ''Computing for theta=''; theta
RE = 0: IM = 0
K = K + 1
'Integration over aperture
FOR I = 1 TO 101
FOR J = 1 TO 101
X = Cw * (51 - I) / 100: Y = Dw * (51 - J) / 100
psi = (2 * PI * X / wavelength) * SIN(theta * PI / 180) * COS(phi * PI / 180)
psi = psi + (2 * PI * Y / wavelength) * SIN(theta * PI / 180) * SIN(phi * PI / 180)
RE = RE + A(I, J) * COS(psi)
IM = IM + A(I, J) * SIN(psi)
NEXT J
```

Figure 14. Computer program to compute the radiation pattern from a circular aperture.

```
NEXT I
TMM = Cp * SQR(RE ^ 2 + IM ^ 2) / reference
IF TMM = 0 THEN TMM = 10 ^ -6
IF theta = 0 THEN
G0DB = 20 * LOG(TMM) / LOG(10): GV = TMM
END IF
pattern(K) = 20 * LOG(TMM) / LOG(10)
NEXT theta
K = 0
FOR theta = 0 TO 10 STEP .1
K = K + 1
PRINT #1, theta, pattern(K)
PRINT ''Angl='': theta; ''E = ''; pattern(K)
NEXT theta
Print ''''
PRINT ''Peak Gain G0 (dB)='': G0DB; '' G0(voltage)='': GV; '' G0(power)='': GV ^ 2
CLOSE #1
END
```

Figure 14 (*Continued*)

transform pair was defined for a line source relating the aperture distribution and the far-field radiation pattern, and vice versa. In the synthesis process, we wish to determine the aperture distribution for a desired radiation pattern. To do this we first express the illumination function as a sum of N uniform distributions:

$$E(x) = \sum_{m=1}^{N} c_m e^{j\phi_m x} \tag{33}$$

The Fourier transform can then be written as

$$E(\theta) = \int_{-L_w}^{L_w} \sum_{m=1}^{N} c_m e^{j(k \sin\theta + \phi_m)x}\, dx \tag{34}$$

yielding for a line source of length L_w

$$E(\theta) = \sum_{m=1}^{N} C_m \frac{\sin\left((k \sin\theta + \phi_m)\dfrac{L_w}{2}\right)}{(k \sin\theta + \phi_m)\dfrac{L_w}{2}} \tag{35}$$

Thus each coefficient C_m is responsible for a $(\sin x)/x$ type of

Table 2. Radiation Pattern Characteristics Produced by Various Circular Aperture Distributions

Distribution	Comments	Normalized Half-Power Beam Width (deg) HPbw/K	Normalized Null-to-Null Beam Width (deg) NULLbw*/K	Side-Lobe Level (dB): SLL dB	Normalized Side-Lobe Angle (deg) SLpos/K	Gain Relative to Uniform (dB) G0 dB	Power Gain Factor Relative to Uniform G0 power	Voltage Gain Factor Relative to Uniform G0 volts
Uniform		59.33	140.00	−17.66	93.67	0.00	1.000	1.000
Cosine raised to power n	$n = 1$	74.67	194.67	−26.07	119.33	−1.42	0.721	0.849
	$n = 2$	88.00	250.00	−33.90	145.50	−2.89	0.514	0.717
	$n = 3$	99.33	306.67	−41.34	173.00	−4.04	0.394	0.628
	$n = 4$	110.00	362.67	−48.51	200.30	−4.96	0.319	0.564
	$n = 5$	120.00	420.00	−55.50	228.17	−5.73	0.267	0.517
Cosine on a pedestal p	$p = 0.0$	74.67	194.67	−26.07	119.33	−1.42	1.000	1.000
	$p = 0.1$	70.67	183.33	−25.61	112.67	−0.98	0.799	0.894
	$p = 0.2$	68.67	174.00	−24.44	107.83	−0.66	0.859	0.927
	$p = 0.3$	66.00	166.00	−23.12	104.17	−0.43	0.905	0.951
	$p = 0.4$	64.67	159.60	−21.91	101.33	−0.27	0.9388	0.9689
	$p = 0.5$	63.33	154.67	−20.85	99.47	−0.17	0.963	0.981
	$p = 0.6$	62.00	150.67	−19.95	97.83	−0.09	0.9789	0.9894
	$p = 0.7$	61.33	147.33	−19.18	96.47	−0.05	0.9895	0.9947
	$p = 0.8$	60.67	144.00	−18.52	95.27	−0.02	0.9958	0.9979
	$p = 0.9$	60.00	142.00	−17.96	94.57	−0.00	0.9991	0.9995
	$p = 1.0$	59.33	140.00	−17.66	93.67	0.00	1.000	1.000
Parabolic raised to power n	$n = 0$	59.33	140	−17.66	93.67	0.00	1.00	1.00
	$n = 1$	72.67	187.33	−24.64	116.33	−1.244	0.701	0.866
	$n = 2$	84.67	232.67	−30.61	138.67	−2.547	0.556	0.746
	$n = 3$	94.67	277.2	−35.96	160.17	−3.585	0.438	0.662
	$n = 4$	104	320.33	−40.91	181.33	−4.432	0.36	0.6

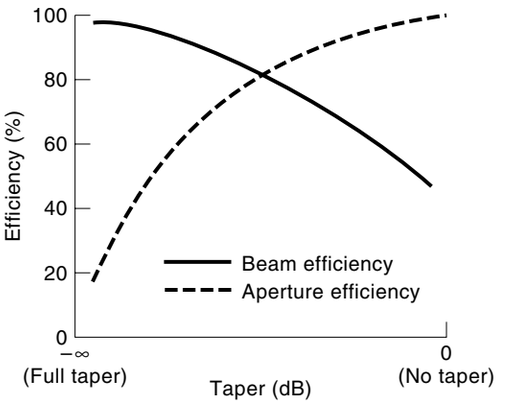

Figure 15. Form of beam and aperture efficiencies for an aperture as a function of taper.

beam, and there are N beams. The coefficients may be obtained manually by estimating the number of independent beams and their relative magnitudes and positions to approximate the desired radiation pattern. Alternatively they may be obtained mathematically via a Fourier-series representation. Also, the results may be extended by the reader to a two-dimensional aperture.

The preceding equations form the basis for Woodward's aperture synthesis technique (6,29) that enables the aperture illumination required to produce a given beam shape to be approximated. A new array antenna synthesis method, called the virtual array synthesis method, was recently published by Vaskelainen (23). In this method, the excitation values of a virtual array are synthesized using some known synthesis method. The geometry of the virtual array can be chosen so that there will be a suitable synthesis method for that geometry, and the synthesis of the virtual array can be done accurately enough. In the synthesis method, the excitation values of the virtual array are transformed into the excitation values of the actual array geometry. Matrix operations are simple and large arrays can be easily synthesized. Further references on recent synthesis techniques appear in Refs. 24 to 28.

BIBLIOGRAPHY

1. D. J. Kozakoff, *Analysis of Radome Enclosed Antennas,* Norwood, MA: Artech House, 1997.
2. S. A. Schelkunoff, Some equivalence theorems of electromagnetics and their application to radiation problems, *Bell System Tech. J.,* **15**: 92–112, 1936.
3. C. Huygens, *Traite de La Lumiere,* Leyden, 1690. Translated into English by S. P. Thompson, Chicago: Univ. Chicago Press, 1912.
4. J. D. Kraus and K. R. Carver, *Electromagnetics,* 2nd ed., New York: McGraw-Hill, pp. 464–467.
5. C. A. Balanis, *Antenna Theory Analysis and Design,* New York: Harper and Row, 1982.
6. A. D. Oliver, Basic Properties of Antennas, in A. W. Rudge et al. (eds.), *The Handbook of Antenna Design,* IEE Electromagnetic Wave Series UK, London: UK, Peter Peregrinum, 1986, chap. 1.
7. H. Jasik, Fundamentals of Antennas, in R. C. Johnson (ed.), *Antenna Engineer Handbook,* 3rd ed., New York: McGraw-Hill, 1993.
8. J. D. Kraus, *Antennas,* 2nd ed., New York: McGraw-Hill, 1988.
9. C. Huygens, *Traite de la Lumiere,* Leyden, 1690; Max Born, *Optik,* Berlin: Springer-Verlag, 1933.
10. A. Sommerfeld, Theorie der Beugung, in P. Frank and R. von Mises (eds.), *Die Differential und Integralgleichungen der Mechanik und Physik,* Braunschweig: Vieweg, 1935.
11. J. D. Kraus, *Radio Astronomy,* 2nd ed., New York: Cygnus-Quasar, 1986.
12. R. E. Collin and Z. J. Zucker, *Antenna Theory,* New York: McGraw-Hill, 1969.
13. W. L. Weeks, *Antenna Engineering,* New York: McGraw-Hill, 1968.
14. T. A. Milligan, *Modern Antenna Design,* New York: McGraw-Hill, 1985.
15. A. W. Rudge et al., *The Handbook of Antenna Design,* Stevenage, UK: Peregrinus, 1986.
16. S. Silver, *Microwave Antenna Theory and Design,* New York: McGraw-Hill, 1949.
17. H. G. Booker and P. C. Clemmow, The concept of an angular spectrum of plane waves and its relation to that of polar diagram and aperture distribution, *Proc. IEE, London, Ser. 3,* **97**: 11–17, 1950.
18. D. R. Rhodes, The optimum line source for the best mean square approximation to a given radiation pattern, *IEEE Trans. Antennas Propag.,* **AP-11**: 440–446, 1963.
19. R. S. Elliot, *Antenna Theory and Design,* Englewood Cliffs, NJ: Prentice-Hall, 1987.
20. I. S. Sokolnikoff and R. M. Redhefer, *Mathematics of Physics and Modern Engineering,* New York: McGraw-Hill, 1958.
21. R. C. Hansen, Linear Arrays, in A. W. Rudge et al. (eds.), *The Handbook of Antenna Design,* Stevenage, UK: Peregrinus, 1986.
22. R. T. Nash, Beam efficiency limitations for large antennas, *IEEE Trans. Antennas Propag.,* **AP-12**: 918–923, 1964.
23. L. I. Vaskelainen, Virtual array synthesis method for planar array antennas, *IEEE Trans. Antennas Propag.,* **46**: 922–928, 1998.
24. R. J. Mailoux, *Phased Array Antenna Handbook,* Norwood, MA: Artech House, 1994.
25. E. Botha and D. A. McNamara, A contoured beam synthesis technique for planar antenna arrays with quadrantal and centrosymmetry, *IEEE Trans. Antennas Propag.,* **41**: 1222–1231, 1993.
26. B. P. Ng, M. H. Er, and C. Kot, A flexible array synthesis method using quadratic programming, *IEEE Trans. Antennas Propag.,* **41**: 1541–1550, 1993.
27. H. J. Orchard, R. S. Elliott, and G. J. Stern, Optimizing the synthesis of shaped beam antenna patterns, *IEE Proc. H,* **132** (1): 63–68, 1985.
28. R. F. E. Guy, General radiation-pattern synthesis technique for array antennas of arbitrary configuration and element type, *Proc. Inst. Electron. Eng.,* **135**, Pt. H, No. 4: 241–248, 1988.
29. P. M. Woodward, A method of calculating the field over a plane aperture required to produce a given polar diagram, *IEE J., UK,* Part III A, **93**: 1554–1558, London, 1947.

Reading List

Baker and Copson, *The Mathematical Theory of Huygens' Principle,* New York: Oxford University Press, 1939.

C. A. Balanis, *Antenna Theory Analysis and Design,* New York: Harper & Row, 1982.

E. T. Bayliss, Design of monopulse difference patterns with low sidelobes, *Bell Syst., Tech. J.,* **47**: 623–650, 1968.

R. N. Bracewell, Tolerance theory of large antennas, *IRE Trans. Antennas Propag.,* **AP-9**: 49–58, 1961.

W. N. Christiansen and J. A. Hogbom, *Radiotelescopes,* Cambridge, UK: Cambridge Univ. Press, 1985.

C. L. Dolph, A current distribution for broadside arrays which optimizes the relationship between the beamwidth and the sidelobe level, *Proc. IRE,* **34**: 335–348, 1946.

R. C. Hansen, A one parameter circular aperture with narrow beamwidth and low sidelobe levels, *IEEE Trans. Antennas Propag.,* **AP-24**: 477–480, 1976.

R. C. Hansen, *Microwave Scanning Antennas,* New York: Academic Press, 1966.

R. C. Hansen, Tables of Taylor distributions for circular aperture antennas, *IRE Trans. Antennas Propag.* **AP-8**: 23–26, 1960.

R. F. Hyneman, A technique for the synthesis of line source antenna patterns having specified sidelobe behavior, *IEEE Trans. Antennas Propag.,* **AP-16**: 430–435, 1968.

H. Jasik, Fundamentals of Antennas, in R. C. Johnson (ed.), *Antenna Engineering Handbook,* 3rd ed., New York: McGraw-Hill, 1993.

J. D. Kraus, *Radio Astronomy,* 2nd ed., New York: Cygnus-Quasar, 1986.

R. T. Nash, Beam efficiency limitations of large antennas, *IEEE Trans. Antennas Propag.,* **AP-12**: 918–923, 1964.

J. F. Ramsay, Fourier transforms in aerial theory, *Marconi Rev.,* **10**: 17, 41, 81, 157, 1947.

J. F. Ramsay, Fourier transforms in aerial theory, *Marconi Rev.,* **9**: 139, 1946.

D. R. Rhodes, *Synthesis of Planar Antenna Sources,* London: Oxford Univ. Press, 1974.

J. Ruze, Physical limitations of antennas, *MIT Research Laboratory Electronic Technical Report No. 248,* 1952.

S. A. Schelkunoff, Some equivalence theorences of electromagnetics and their application to radiation problems, *Bell Syst. Tech. J.,* **15**: 92–112, 1936.

H. E. Shanks, A geometrical optics method of pattern synthesis for linear arrays, *IRE Trans. Antennas Propag.,* **AP-8**: 485–490, 1960.

M. I. Skolnik, *Introduction to Radar Systems,* 2nd ed., New York: McGraw-Hill, 1980.

J. C. Slater and N. H. Frank, *Introduction to Theoretical Physics,* New York: McGraw-Hill, 1933.

T. T. Taylor, Design of circular apertures for narrow beamwidth and low sidelobe levels, *IEEE Trans. Antennas Propag.,* **AP-8**: 17–22, 1960.

T. T. Taylor, Design of line-source antennas for narrow beamwidth and low sidelobes, *IRE Trans. Antennas Propag.,* **AP-3**: 16–28, 1955.

I. Wolf, Determination of the radiating system which will produce a specified directional characteristic, *Trans. IRE,* **25**: 630–643, 1937.

P. M. Woodward, A method of calculating the field over a plane aperture required to produce a given polar diagram, *IEE J.,* Part III A, **93**: 1554–1558, 1947.

P. M. Woodward and J. D. Lawson, The theoretical precision with which an arbitrary radiation pattern may be obtained from a source of a finite size, *IEE J.,* Part III, **95**: 363–370, 1948.

DENNIS KOZAKOFF
Millimeter Wave Technology

APPARATUS, RADIOLOGICAL IMAGING. See X-RAY APPARATUS.

APPARATUS, X-RAY IMAGING. See X-RAY APPARATUS.

APPLIANCES, DOMESTIC. See DOMESTIC APPLIANCES.

APPLICATION FRAMEWORKS. See USER INTERFACE MANAGEMENT SYSTEMS.